



intensity. This value is more robust than the intensities of the colonies and allows us to work in the gray level domain. The conversion from the RGB image to a gray level image is based on the weighted sum of the RGB values given by  $I_{\text{gray}} = 0.30 R + 0.59 G + 0.11 B$ .

Marker and manufacturer annotations are darker than the colonies and the nourishment medium. In any Petri dish image with annotations, there are three distinct regions: Cell colonies, agar medium and annotations. Thus it can be assumed that the histogram of the normalized gray level image is trimodal (Fig. 2). The leftmost peak of the histogram, representing the darker gray levels of the image are contributed almost completely by annotations. Cell colonies populate the middle regions of the histogram while the agar medium fills the brighter part of the histogram.

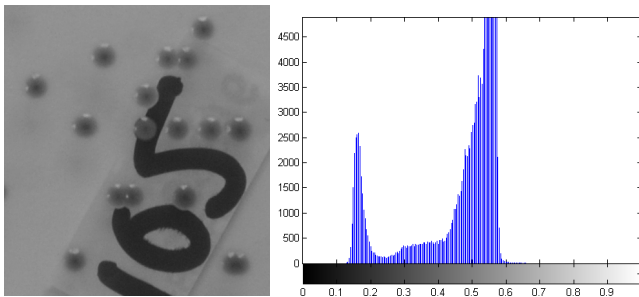


Figure 2. Marked image (left) and associated gray level histogram (right).

Assuming that each region has a Gaussian distribution histogram, Gaussian fitting techniques can be used to extract the mask of the annotation area. With an Expectation-Maximization step, we can estimate each Gaussian parameter and establish safe thresholding values to segment the annotation mask (Fig. 3).

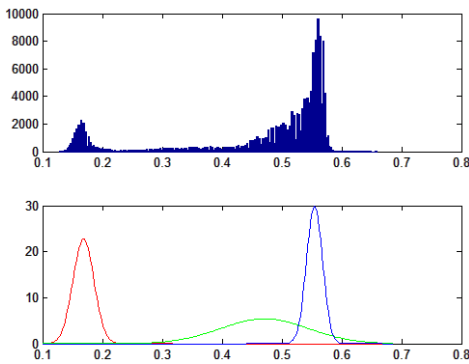


Figure 3. Tri-modal histogram and three fitted Gaussians using the Expectation Maximization algorithm. Red: Gaussian annotations, green: agar colonies, blue: agar medium.

The thresholding value  $\tau$  for the mask section is calculated as:

$$\tau = \min(\mu_3 + 3\sigma_3, 0.3)$$

where  $\sigma_3$  and  $\mu_3$  are the standard deviation and mean of parameters of the Gaussian representing the annotations.

Since some bacterial colony fragments may appear into the masked area, as some may have dark areas under certain illumination conditions, the mask has to be cleaned of these non marker areas. The colony fragments that are included after thresholding the image are smaller than marker annotations, so region analysis can be used to discard the unwanted regions (typically smaller than the average colony size).

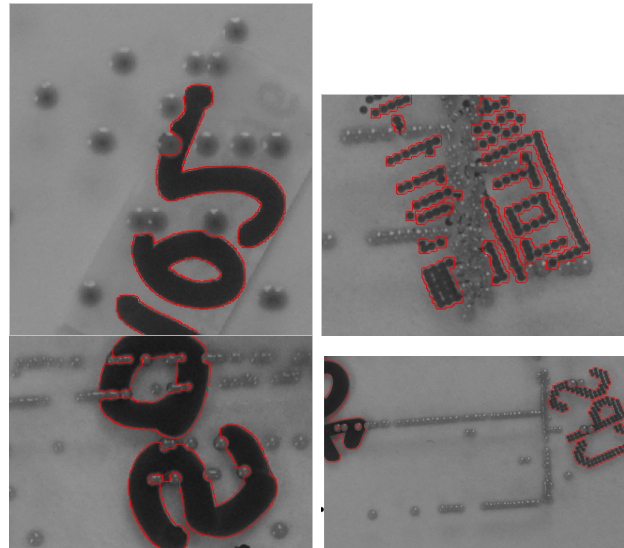


Figure 4. Thresholded masks of the annotations.

### B. Image inpainting

Inpainting is a technique used to remove unwanted objects from an image or to correct small defects and glitches in old or deteriorated images. In the digital era, automated algorithms for image inpainting (also known as image interpolation) have been developed that work by propagating information inwards, from the boundary of the region to recover.

The reference work of image inpainting [4] uses isophotes (lines with the same image intensity) to propagate the information inwards. Isophotes are calculated using the discretized gradient. This technique is slow and works best in small inpainted areas. Our mask is relatively big and the gradients in the nourishment medium of the plate low. This method was unable to reconstruct a suitable image in a reasonable time in our tests, as shown in Fig. 5 (left). Other inpaint techniques such as [5] combine texture and gradient information to fill the image gaps. However, given the lack of texture information in the agar medium area, this method can generate artifacts when filling the marked areas as exemplified in Fig. 5 (right). Poisson based inpainting [6], uses gradient information to seamlessly copy areas from two images, but defaults to Laplace inpainting when no gradient information is available. Low gradient, textureless area like agar medium, can be interpolated better with only gray level information as there is almost no structure information in the medium.

This allows the utilization of faster methods that handle the problem correctly.

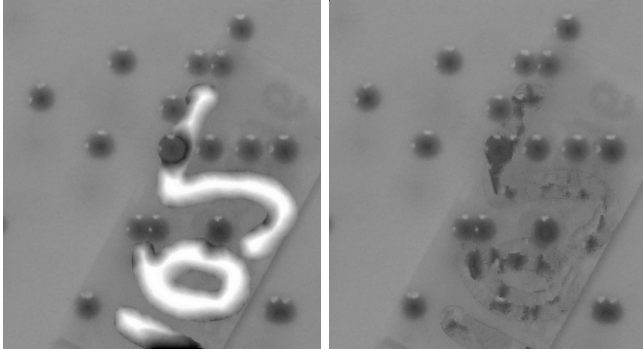


Figure 5. Discarded methods. Isophote based inpainting is unable to fill the whole region (left). Texture based inpainting is unable to interpolate correctly the marker area (right).

Our inpainting method propagates the gray level information at the borders using discretised Partial Differential Equations (PDE). The gray levels of the boundary of the region are used as boundary condition to the PDE. Its values are used to calculate the immediate unknown pixels and the information is propagated inwards. This way the information can be propagated to relatively long distances and because of the structure of the image, the resulting image is free of artifacts.

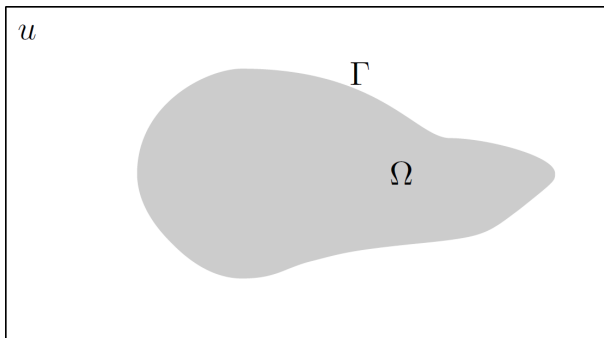


Figure 6. The image  $u$  has an unknown region  $\Omega$ . The values inside  $\Omega$  have to be calculated with the values along the boundary  $\Gamma$ .

Given an image function  $u$  and  $\Omega \subset u$ , we want to estimate the values inside  $\Omega$ . The problem can be solved using the Laplace equation  $\nabla^2(u) = 0$  at each unknown point given the Dirichlet boundary condition imposed by the known values of  $u$  at the boundary of  $\Omega$ ,  $\Gamma = \partial\Omega$  (Fig. 6).

The PDE can be solved by finite difference methods. This requires a discretisation of the domain  $\Omega$  and the Laplace equation governing it. The domain is sampled at regular steps  $\delta x, \delta y$  (with  $\delta x = \delta y$ ) and each sample  $u_{i,j}$  is connected with its Von Neumann neighbourhood. In this grid, the Laplace equation can be discretised using second order central finite differences for both directional derivatives  $\Delta_{xx}, \Delta_{yy}$  as

follows:

$$\frac{u_{i+1,j} - 2u_{i,j} + u_{i-1,j}}{\delta x^2} + \frac{u_{i,j+1} - 2u_{i,j} + u_{i,j-1}}{\delta y^2} = 0.$$

The full set of discrete equation with the constraints imposed by the boundary conditions define a system of sparse linear equations that can be solved using standard relaxation methods like Jacobi or Gauss Seidel.

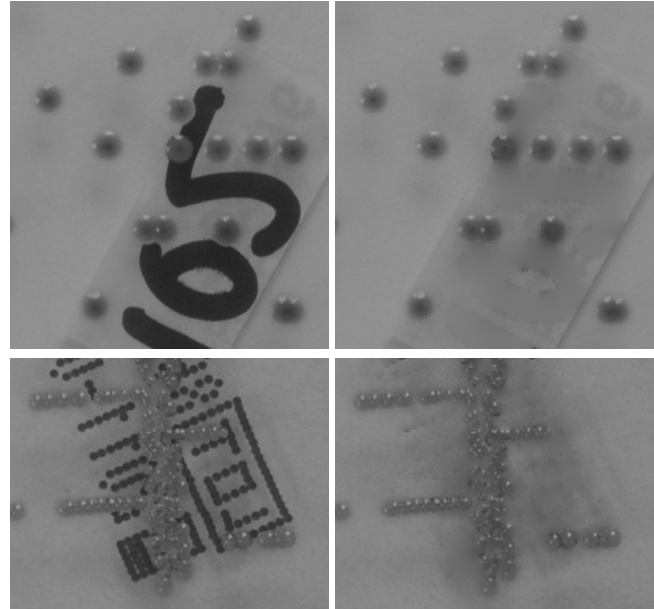


Figure 7. PDE-based interpolation of values produces artifact-free inpainting in our test images.

With the markers removed (Fig. 7), cell segmentation algorithms can be used to isolate individual cell colonies and perform the counting. In our implementation we use the gold standard method of watershed-based segmentation, given its strength at identifying partially merged colonies [7], [8].

### III. RESULTS

Experiments have been run using seven images of Petri dishes with colonies of different bacteria types: *Escherichia coli*, *Enterococcus*, *Staphylococcus* and *Klebsiella*. All dishes had both marker and manufacturer annotations on the back. Image resolution is over 4.5 Megapixels in all cases. Given their size, each of the original images are cut into 25 smaller rectangular images. From the 175 sub-images we discarded 17 images where bacterial colonies were so merged that they formed a uniform surface (bacterial lawn) as shown in Fig. 8. Detection of such dense populated areas requires a completely different approach, based on estimating the density and total area of the area covered by colonies. The final set of 158 sub-images include different degrees of bacterial colonies numbers, from low number of isolated colonies – Fig. 9 (upper row)– to areas with clusters of merged colonies – Fig. 9 (lower row)–. Results indicate a clear improvement in the reduction of false positives in the images, especially

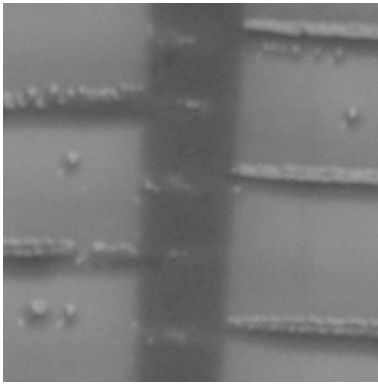


Figure 8. Colonies merged into bacterial lawn.

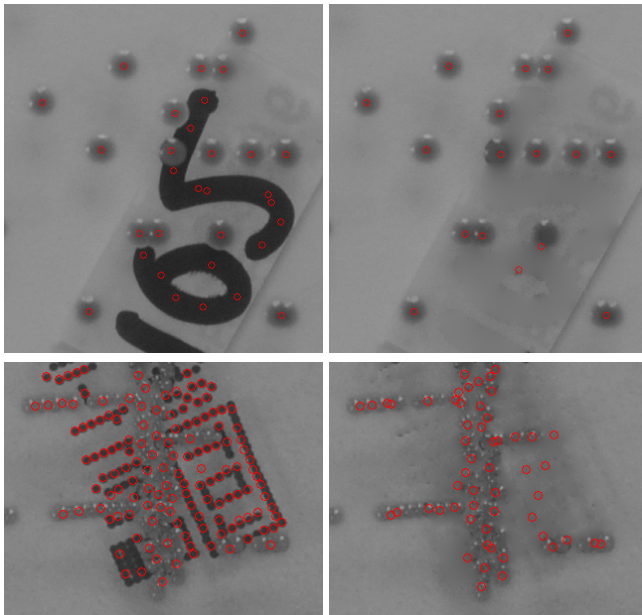


Figure 9. Counting results in original images (left) and corrected images (right). Annotation removal improves detection rate by lowering the ratio of false positive detections, especially when manufacturer marks can be interpreted as colonies (lower row).

with the case of manufacturer annotations (composed of small black circles with size comparable to the manufacturer annotations) that are easily detected as cell colonies. An example is shown in Fig. 9 (lower row). The annotations have a size comparable with the colonies so the number of false positives is very high. Removal of annotations yields a number of detected colonies much closer to the real number. Results are improved in 91.7% of the sub-images. Images where the removal of annotations produces worse results are those with dense clusters of bacterial colonies (but not forming bacterial lawn). In such images, the counting algorithm underestimates the number of colonies, and the presence of marker annotations increases the estimated value, resulting in an amount of detected colonies closer to the real value.

Additionally, given that our images were not captured with

a complete control of illumination, a shadow appears around some of the annotations. This darker shadow is not included in the mask and generates darker areas in the inpainted image, that although unpleasant to the eye still allows the counting algorithm to obtain better results. Also colonies near the edges of inpainted zones can reflect some of the darker colors of the marker zones. This results in interpolated areas that are darker than the medium.

#### IV. CONCLUSIONS

Annotations in Petri dishes are present in a great number of microbiology laboratories. Any automated bacterial colony counting system needs to take into account the presence of such image feature that interferes with normal processing of images. The presented method, based on the automatic detection and inpainting of the annotated area, improves the results of automated colony counter systems by lowering the false positives related with erroneous classifications of annotations as colonies due to the presence of these elements in the images.

#### REFERENCES

- [1] UVP L.L.C., "Colonydoc-it imaging station," 2011, <http://www.uvp.com/colony.html>.
- [2] IUL Instruments S.A., "Flash and go automated colony counter," 2011, <http://www.iul-inst.com>.
- [3] G. Corkidi, R. Diaz-Urbe, J. L. Folch-Mallol, and J. Nieto-Sotelo, "Covasiem: an image analysis method that allows detection of confluent microbial colonies and colonies of various sizes for automated counting," *Applied and Environmental Microbiology*, vol. 64, no. 4, pp. 1400–1404, 1998.
- [4] M. Bertalmio, G. Sapiro, V. Caselles, and C. Ballester, "Image inpainting," in *Proceedings of the 27th annual conference on Computer Graphics and Interactive Techniques*, 2000, pp. 417–424.
- [5] A. Criminisi, P. Pérez, and K. Toyama, "Region filling and object removal by exemplar-based image inpainting," *IEEE transactions on image processing : a publication of the IEEE Signal Processing Society*, vol. 13, no. 9, pp. 1200–12, Sept. 2004.
- [6] P. Pérez, M. Gangnet, and A. Blake, "Poisson image editing," in *ACM SIGGRAPH 2003 Papers*, ser. SIGGRAPH '03. ACM, 2003, pp. 313–318.
- [7] C. Zhang, W.-B. Chen, W.-L. Liu, and C.-B. Chen, "An automated bacterial colony counting system," *2008 IEEE International Conference on Sensor Networks, Ubiquitous, and Trustworthy Computing*, pp. 233–240, 2008.
- [8] H. Ateş, "An image-processing based automated bacteria colony counter," *2009 24th International Symposium on Computer and Information Sciences*, pp. 18–23, 2009.